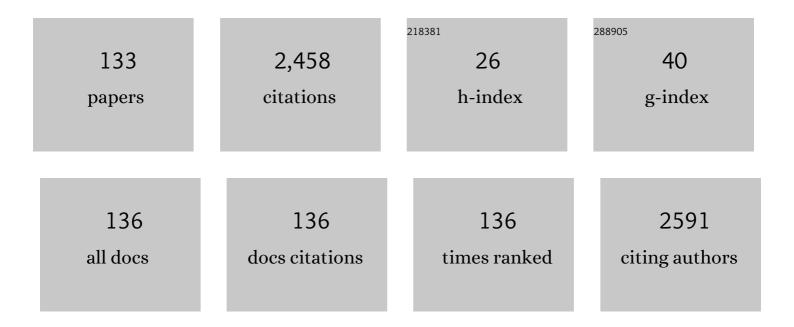
Joan Josep Roa Rovira

List of Publications by Year in descending order

Source: https://exaly.com/author-pdf/5955993/publications.pdf Version: 2024-02-01



#	Article	IF	CITATIONS
1	Mechanical properties at the nanometer scale of GDC and YSZ used as electrolytes for solid oxide fuel cells. Acta Materialia, 2010, 58, 2504-2509.	3.8	100
2	Study of the recycled aggregates nature's influence on the aggregate–cement paste interface and ITZ. Construction and Building Materials, 2014, 68, 677-684.	3.2	83
3	A review of doped lanthanum gallates as electrolytes for intermediate temperature solid oxides fuel cells: From materials processing to electrical and thermo-mechanical properties. Journal of the European Ceramic Society, 2016, 36, 1-16.	2.8	76
4	Intrinsic hardness of constitutive phases in WC–Co composites: Nanoindentation testing, statistical analysis, WC crystal orientation effects and flow stress for the constrained metallic binder. Journal of the European Ceramic Society, 2015, 35, 3419-3425.	2.8	68
5	Effect of shot peening on metastable austenitic stainless steels. Materials Science & Engineering A: Structural Materials: Properties, Microstructure and Processing, 2015, 641, 290-296.	2.6	66
6	Hall-Petch strengthening of the constrained metallic binder in WC–Co cemented carbides: Experimental assessment by means of massive nanoindentation and statistical analysis. Materials Science & Engineering A: Structural Materials: Properties, Microstructure and Processing, 2016, 676, 487-491.	2.6	66
7	Calculation of Young's Modulus Value by Means of AFM. Recent Patents on Nanotechnology, 2011, 5, 27-36.	0.7	63
8	Mapping of mechanical properties at microstructural length scale in WC-Co cemented carbides: Assessment of hardness and elastic modulus by means of high speed massive nanoindentation and statistical analysis. International Journal of Refractory Metals and Hard Materials, 2018, 75, 211-217.	1.7	54
9	Dependence of nanoindentation hardness with crystallographic orientation of austenite grains in metastable stainless steels. Materials Science & Engineering A: Structural Materials: Properties, Microstructure and Processing, 2015, 645, 188-195.	2.6	50
10	Mechanical Properties of 3D-Printing Polylactic Acid Parts subjected to Bending Stress and Fatigue Testing. Materials, 2019, 12, 3859.	1.3	49
11	Nanohardness and Young's modulus of YBCO samples textured by the Bridgman technique. Nanotechnology, 2007, 18, 385701.	1.3	47
12	Fracture and fatigue behavior of WC–Co and WC–CoNi cemented carbides. International Journal of Refractory Metals and Hard Materials, 2015, 49, 184-191.	1.7	46
13	Hardness and Young's modulus distributions in atmospheric plasma sprayed WC–Co coatings using nanoindentation. Surface and Coatings Technology, 2011, 205, 4192-4197.	2.2	45
14	Contact damage and fracture micromechanisms of multilayered TiN/CrN coatings at micro- and nano-length scales. Thin Solid Films, 2014, 571, 308-315.	0.8	42
15	The effects of bimodal grain size distributions on the work hardening behavior of a TRansformation-TWinning induced plasticity steel. Materials Science & Engineering A: Structural Materials: Properties, Microstructure and Processing, 2016, 678, 23-32.	2.6	41
16	Structural and mechanical characterization of graphite foam/phase change material composites. Carbon, 2014, 74, 266-281.	5.4	40
17	Nanosecond-laser patterning of 3Y-TZP: Damage and microstructural changes. Journal of the European Ceramic Society, 2017, 37, 4876-4887.	2.8	40
18	Enhanced thermal stability and fracture toughness of TiAlN coatings by Cr, Nb and V-alloying. Surface and Coatings Technology, 2018, 342, 85-93.	2.2	40

JOAN JOSEP ROA ROVIRA

#	Article	IF	CITATIONS
19	Nanoindentation and fracture toughness of nanostructured zirconia/multi-walled carbon nanotube composites. Ceramics International, 2015, 41, 2453-2461.	2.3	37
20	Hydrofluoric acid etching of dental zirconia. Part 1: etching mechanism and surface characterization. Journal of the European Ceramic Society, 2016, 36, 121-134.	2.8	37
21	Processing of graded anode-supported micro-tubular SOFCs based on samaria-doped ceria via gel-casting and spray-coating. Ceramics International, 2012, 38, 3713-3722.	2.3	34
22	Depth-sensing indentation applied to polymers: A comparison between standard methods of analysis in relation to the nature of the materials. European Polymer Journal, 2013, 49, 4047-4053.	2.6	32
23	Coefficient of friction and wear resistance of zirconia–MWCNTs composites. Ceramics International, 2015, 41, 459-468.	2.3	32
24	Mechanical deformation of WC–Co composite micropillars under uniaxial compression. International Journal of Refractory Metals and Hard Materials, 2016, 54, 70-74.	1.7	32
25	Structure, deformation and fracture of arc evaporated Zr–Si–N hard films. Surface and Coatings Technology, 2014, 258, 1100-1107.	2.2	31
26	Micromechanical properties of WC-(W,Ti,Ta,Nb)C-Co composites. Journal of Alloys and Compounds, 2019, 777, 593-601.	2.8	30
27	Study of the friction, adhesion and mechanical properties of single crystals, ceramics and ceramic coatings by AFM. Journal of the European Ceramic Society, 2011, 31, 429-449.	2.8	26
28	Nanoindentation with spherical tips of single crystals of YBCO textured by the Bridgman technique: Determination of indentation stress–strain curves. Journal of the European Ceramic Society, 2010, 30, 1477-1482.	2.8	25
29	Performance of a novel type of electrolyte-supported solid oxide fuel cell with honeycomb structure. Journal of Power Sources, 2010, 195, 516-521.	4.0	25
30	AFM as an alternative for Young's modulus determination in ceramic materials in elastic deformation regime. Physica C: Superconductivity and Its Applications, 2011, 471, 544-548.	0.6	25
31	Experimental Correlation of Mechanical Properties of the Ti-6Al-4V Alloy at Different Length Scales. Metals, 2021, 11, 104.	1.0	25
32	Deformation mechanisms induced under high cycle fatigue tests in a metastable austenitic stainless steel. Materials Science & Engineering A: Structural Materials: Properties, Microstructure and Processing, 2014, 597, 232-236.	2.6	24
33	Deformation mechanisms induced by nanoindentation tests on a metastable austenitic stainless steel: A FIB/SIM investigation. Materials Characterization, 2017, 131, 253-260.	1.9	24
34	Grinding-induced metallurgical alterations in the binder phase of WC-Co cemented carbides. Materials Characterization, 2017, 134, 302-310.	1.9	24
35	Novel Mechanical Characterization of Austenite and Ferrite Phases within Duplex Stainless Steel. Metals, 2020, 10, 1352.	1.0	24
36	Corrosion damage in WC–Co cemented carbides: residual strength assessment and 3D FIB-FESEM tomography characterisation. Powder Metallurgy, 2014, 57, 324-330.	0.9	23

#	Article	IF	CITATIONS
37	Berkovich nanoindentation and deformation mechanisms in a hardmetal binder-like cobalt alloy. Materials Science & Engineering A: Structural Materials: Properties, Microstructure and Processing, 2015, 621, 128-132.	2.6	23
38	Correlation between electrical and mechanical properties in La1â^'xSrxGa1â^'yMgyO3â^'δ ceramics used as electrolytes for solid oxide fuel cells. Journal of Power Sources, 2014, 246, 918-925.	4.0	22
39	Influence of pre-existing martensite on the wear resistance of metastable austenitic stainless steels. Wear, 2016, 364-365, 40-47.	1.5	22
40	Substrate surface finish effects on scratch resistance and failure mechanisms of TiN-coated hardmetals. Surface and Coatings Technology, 2015, 265, 174-184.	2.2	21
41	The influence of unshielded small cracks in the fracture toughness of yttria and of ceria stabilised zirconia. Journal of the European Ceramic Society, 2016, 36, 147-153.	2.8	21
42	Characterization of interfaces between TiCN and iron-base binders. International Journal of Refractory Metals and Hard Materials, 2017, 63, 32-37.	1.7	21
43	Determination of hardness, Young's modulus and fracture toughness of lanthanum tungstates as novel proton conductors. Ceramics International, 2011, 37, 1593-1599.	2.3	20
44	Nanoindentation of multilayered epitaxial YBa2Cu3O7-Î′ thin films and coated conductors. Thin Solid Films, 2011, 519, 2470-2476.	0.8	20
45	Plastic deformation and damage induced by fatigue in TWIP steels. Materials Science & Engineering A: Structural Materials: Properties, Microstructure and Processing, 2015, 628, 410-418.	2.6	20
46	Surface grain size and texture after annealing ground zirconia. Journal of the European Ceramic Society, 2016, 36, 1519-1525.	2.8	20
47	Performance and short-term stability of single-chamber solid oxide fuel cells based on La0.9Sr0.1Ga0.8Mg0.2O3â~δ electrolyte. Journal of Power Sources, 2012, 216, 417-424.	4.0	19
48	Correlation Between Microstructure and Mechanical Properties Before and After Reversion of Metastable Austenitic Stainless Steels. Metallurgical and Materials Transactions A: Physical Metallurgy and Materials Science, 2015, 46, 5697-5707.	1.1	19
49	Mechanical properties of 12Ce–ZrO2/3Y–ZrO2 composites. Ceramics International, 2015, 41, 14988-14997.	2.3	19
50	Deformation of polycrystalline TRIP stainless steel micropillars. Materials Science & Engineering A: Structural Materials: Properties, Microstructure and Processing, 2015, 647, 51-57.	2.6	19
51	Scale effect in mechanical characterization of WC-Co composites. International Journal of Refractory Metals and Hard Materials, 2018, 72, 157-162.	1.7	19
52	Manufacturing of anode-supported tubular solid oxide fuel cells by a new shaping technique using aqueous gel-casting. Journal of Power Sources, 2012, 200, 45-52.	4.0	18
53	The sequential twinning-transformation induced plasticity effects in a thermomechanically processed high Mn austenitic steel. Materials Science & Engineering A: Structural Materials: Properties, Microstructure and Processing, 2018, 725, 242-249.	2.6	18
54	Study of the mechanical properties of CeO2 layers with the nanoindentation technique. Thin Solid Films, 2009, 518, 227-232.	0.8	17

#	Article	IF	CITATIONS
55	Assessment of mechanical properties at microstructural length scale of Ti(C,N)–FeNi ceramic-metal composites by means of massive nanoindentation and statistical analysis. Ceramics International, 2019, 45, 20202-20210.	2.3	17
56	Evolution of microstructure and residual stresses in gradually ground/polished 3Y-TZP. Journal of the European Ceramic Society, 2020, 40, 1582-1591.	2.8	17
57	Mechanical properties at nanometric scale of alumina layers formed in sulphuric acid anodizing under burning conditions. Ceramics International, 2012, 38, 1627-1633.	2.3	16
58	Influence of specimen size and microstructure on uniaxial compression of WC-Co micropillars. Ceramics International, 2019, 45, 15934-15941.	2.3	16
59	Design of alternative binders for hard materials. International Journal of Refractory Metals and Hard Materials, 2020, 87, 105089.	1.7	16
60	Influence of the processing route on the properties of Ti(C,N)-Fe15Ni cermets. International Journal of Refractory Metals and Hard Materials, 2020, 87, 105046.	1.7	16
61	Peptidic biofunctionalization of laser patterned dental zirconia: A biochemical-topographical approach. Materials Science and Engineering C, 2021, 125, 112096.	3.8	16
62	Superficial Effects of Ball Burnishing on TRIP Steel AISI 301LN Sheets. Metals, 2021, 11, 82.	1.0	16
63	Mechanical Characterisation at Nanometric Scale of a New Design of SOFCs. Fuel Cells, 2011, 11, 124-130.	1.5	14
64	Anodeâ€supported SOFC Operated Under Singleâ€chamber Conditions at Intermediate Temperatures. Fuel Cells, 2011, 11, 108-115.	1.5	14
65	Chemical milling effect on the low cycle fatigue properties of cast Ti–6Al–2Sn–4Zr–2Mo alloy. International Journal of Fatigue, 2016, 92, 193-202.	2.8	14
66	Small-scale mechanical properties of constitutive phases within a polycrystalline cubic boron nitride composite. Journal of the European Ceramic Society, 2019, 39, 5181-5189.	2.8	14
67	Carbon addition effects on microstructure and small-scale hardness for Ti(C,N)-FeNi cermets. International Journal of Refractory Metals and Hard Materials, 2019, 85, 105064.	1.7	12
68	Improving Mechanical Properties of Glass Fiber Reinforced Polymers through Silica-Based Surface Nanoengineering. ACS Applied Polymer Materials, 2020, 2, 2667-2675.	2.0	12
69	Deformation kinetics of a TRIP steel determined by in situ high-energy synchrotron X-ray diffraction. Materialia, 2021, 20, 101251.	1.3	12
70	Free-Standing Faradaic Motors Based on Biocompatible Nanoperforated Poly(lactic Acid) Layers and Electropolymerized Poly(3,4-ethylenedioxythiophene). ACS Applied Materials & Interfaces, 2019, 11, 29427-29435.	4.0	11
71	Enhanced osteoconductivity on electrically charged titanium implants treated by physicochemical surface modifications methods. Nanomedicine: Nanotechnology, Biology, and Medicine, 2019, 18, 1-10.	1.7	11
72	Remote Spatiotemporal Control of a Magnetic and Electroconductive Hydrogel Network via Magnetic Fields for Soft Electronic Applications. ACS Applied Materials & Interfaces, 2021, 13, 42486-42501.	4.0	11

#	Article	IF	CITATIONS
73	Electrical and mechanical characterization by instrumented indentation technique of La0.85Sr0.15Ga0.8Mg0.2O3â~ electrolyte for SOFCs. Journal of the European Ceramic Society, 2012, 32, 4287-4293.	2.8	10
74	Influence of microstructure and mechanical properties on the tribological behavior of reactive arc deposited Zr-Si-N coatings at room and high temperature. Surface and Coatings Technology, 2016, 304, 393-400.	2.2	10
75	Assessment of corrosion-induced changes on the mechanical integrity of cemented carbides at small length scales. International Journal of Refractory Metals and Hard Materials, 2019, 84, 105033.	1.7	10
76	Nanomechanical Characterization of the Deformation Response of Orthotropic Ti–6Al–4V. Advanced Engineering Materials, 2021, 23, 2001341.	1.6	10
77	ElectroCatalytic Activity of Nickel Foam with Co, Mo, and Ni Phosphide Nanostructures. Plasma, 2022, 5, 221-232.	0.7	10
78	Effective silver-assisted welding of YBCO blocks: mechanical versus electrical properties. Superconductor Science and Technology, 2010, 23, 045013.	1.8	9
79	Annealing aged zirconia: Study of surface mechanical properties at the micrometric length scale. Journal of the European Ceramic Society, 2015, 35, 1031-1039.	2.8	9
80	Nanoindentation and scratch resistance of multilayered TiO2-SiO2coatings with different nanocolumnar structures deposited by PV-OAD. Journal Physics D: Applied Physics, 2016, 49, 135104.	1.3	9
81	WC-base cemented carbides with partial and total substitution of Co as binder: Evaluation of mechanical response by means of uniaxial compression of micropillars. International Journal of Refractory Metals and Hard Materials, 2019, 84, 105027.	1.7	9
82	Influence of grinding/polishing on the mechanical, phase stability and cell adhesion properties of yttria-stabilized zirconia. Journal of the European Ceramic Society, 2020, 40, 4304-4314.	2.8	9
83	Anisotropy effect of bioinspired ceramic/ceramic composites: Can the platelet orientation enhance the mechanical properties at micro- and submicrometric length scale?. Journal of the European Ceramic Society, 2021, 41, 2753-2762.	2.8	9
84	Mechanical properties of highly textured porous Ni–YSZ and Co–YSZ cermets produced from directionally solidified eutectics. Ceramics International, 2011, 37, 3123-3131.	2.3	8
85	Effect of the filler on the nanomechanical properties of polypropylene in contact with paraffinic phase change material. European Polymer Journal, 2015, 63, 29-36.	2.6	8
86	Thermal and mechanical stability of wurtzite-ZrAlN/cubic-TiN and wurtzite-ZrAlN/cubic-ZrN multilayers. Surface and Coatings Technology, 2017, 324, 328-337.	2.2	8
87	Cyclic contact fatigue of cemented carbides under dry and wet conditions: Correlation between microstructure, damage and electrochemical behavior. International Journal of Refractory Metals and Hard Materials, 2020, 92, 105279.	1.7	8
88	3D FIB/FESEM tomography of grinding-induced damage in WC-Co cemented carbides. Procedia CIRP, 2020, 87, 385-390.	1.0	8
89	Mechanical characterization at nanometric scale for heterogeneous graphite–salt phase change materials with a statistical approach. Ceramics International, 2012, 38, 401-409.	2.3	7
90	Influence of laser cutting on the fatigue limit of two high strength steels*. Materialpruefung/Materials Testing, 2015, 57, 136-140.	0.8	7

#	Article	IF	CITATIONS
91	Small scale fracture behaviour of multilayer TiN/CrN systems: Assessment of bilayer thickness effects by means of ex-situ tests on FIB-milled micro-cantilevers. Surface and Coatings Technology, 2016, 308, 414-417.	2.2	7
92	Influence of testing mode on the fatigue behavior of <111> austenitic grain at the nanometric length scale for TRIP steels. Materials Science & Engineering A: Structural Materials: Properties, Microstructure and Processing, 2018, 713, 287-293.	2.6	7
93	Contact fatigue behavior of α-Al2O3-Ti(C,N) CVD coated WC-Co under dry and wet conditions. Materials Letters, 2021, 284, 129012.	1.3	7
94	Influence of microstructural assemblage of the substrate on the adhesion strength of coated PcBN grades. Ceramics International, 2022, 48, 22313-22322.	2.3	7
95	Nanoindentation of Bridgman YBCO samples. Ceramics International, 2012, 38, 2035-2042.	2.3	6
96	Oxygenation kinetics of YBCO-TSMG samples using the nanoindentation technique. Journal of the European Ceramic Society, 2012, 32, 425-431.	2.8	6
97	Mechanical properties of Al2O3 inverse opals by means of nanoindentation. Journal Physics D: Applied Physics, 2016, 49, 455303.	1.3	6
98	Influence of cyclic thermal treatments on the oxidation behavior of Ti-6Al-2Sn-4Zr-2Mo alloy. Materials Characterization, 2018, 145, 218-224.	1.9	6
99	Geometrically Necessary Dislocations on Plastic Deformation of Polycrystalline TRIP Steel. Crystals, 2019, 9, 289.	1.0	6
100	Hybrid conducting alginate-based hydrogel for hydrogen peroxide detection from enzymatic oxidation of lactate. International Journal of Biological Macromolecules, 2021, 193, 1237-1248.	3.6	6
101	Effectiveness of Direct Laser Interference Patterning and Peptide Immobilization on Endothelial Cell Migration for Cardio-Vascular Applications: An In Vitro Study. Nanomaterials, 2022, 12, 1217.	1.9	6
102	Corrosion induced degradation of textured YBCO under operation in high humidity conditions. Surface and Coatings Technology, 2012, 206, 4256-4261.	2.2	5
103	Paramagnetic Meissner effect and strong time dependence at high fields in melt-textured high-T C superconductors. Journal of the Korean Physical Society, 2013, 62, 1414-1417.	0.3	5
104	Phase transformation under thermal fatigue of high Mn-TWIP steel: Microstructure and mechanical properties. Materials Science & Engineering A: Structural Materials: Properties, Microstructure and Processing, 2016, 677, 431-437.	2.6	5
105	Structural and mechanical properties of Zr1â^'x Mox thin films: From the nano-crystalline to the amorphous state. Journal of Alloys and Compounds, 2017, 729, 137-143.	2.8	5
106	Characterization Study of an Oxide Film Layer Produced under CO2/Steam Atmospheres on Two Different Maraging Steel Grades. Metals, 2021, 11, 746.	1.0	5
107	Yield strength, shear stress and toughness of YBCO samples textured by Bridgman technique. Journal of Physics: Conference Series, 2008, 97, 012116.	0.3	4
108	Fracture micromechanisms and mechanical behavior of YBCO bulk superconductors at 77 and 300K. Ceramics International, 2014, 40, 12797-12806.	2.3	4

#	Article	IF	CITATIONS
109	Hardness of FRHC-Cu Determined by Statistical Analysis. Journal of Materials Engineering and Performance, 2014, 23, 637-642.	1.2	4
110	Thermally Induced Surface Integrity Changes of Ground WC-Co Hardmetals. Procedia CIRP, 2016, 45, 91-94.	1.0	4
111	Dynamic Deformation of Metastable Austenitic Stainless Steels at the Nanometric Length Scale. Metallurgical and Materials Transactions A: Physical Metallurgy and Materials Science, 2018, 49, 6034-6039.	1.1	4
112	Contact Mechanics at Nanometric Scale Using Nanoindentation Technique for Brittle and Ductile Materials. Recent Patents on Engineering, 2012, 6, 116-126.	0.3	3
113	Reversible Phase Transformation in Polycrystalline TRIP Steels Induced by Cyclic Indentation Performed at the Nanometric Length Scale. Steel Research International, 2018, 89, 1800234.	1.0	3
114	Synthesis and Characterization of an Fe/Co Ferrite Spinel Oxide Film Produced by Using N2/Steam Heat Treatment on Two Maraging Steels. Metallurgical and Materials Transactions A: Physical Metallurgy and Materials Science, 2022, 53, 1276-1293.	1.1	3
115	Surface integrity of new dry-electropolishing technology on WC-Co cemented carbides. Procedia CIRP, 2022, 108, 543-548.	1.0	3
116	Paramagnetic moments and time effects in melt-textured NdBaCuO system with Nd422 inclusions. Journal of Physics: Conference Series, 2015, 592, 012064.	0.3	2
117	High-field paramagnetic Meissner effect up to 14 T in melt-textured YBa 2 Cu 3 O 7 – Î′. Physica C: Superconductivity and Its Applications, 2016, 525-526, 105-110.	0.6	2
118	Chemical segregation in a 12Ce-ZrO2/3Y-ZrO2 ceramic composite. Materials Characterization, 2017, 132, 83-91.	1.9	2
119	Implementation of advanced characterisation techniques for assessment of grinding effects on the surface integrity of WC–Co cemented carbides. Powder Metallurgy, 2018, 61, 100-105.	0.9	2
120	Chemical and nanoindentation study of diffusion during sintering of 12Ce-ZrO2/3Y-ZrO2 powder layers. Ceramics International, 2018, 44, 2485-2490.	2.3	2
121	Influence of the Crystallographic Orientation on the Yield Strength and Deformation Mechanisms of Austenitic Grains in Metastable Stainless Steels Investigated by Spherical Nanoindentation. Steel Research International, 2019, 90, 1800425.	1.0	2
122	Transmission of Plasticity Through Grain Boundaries in a Metastable Austenitic Stainless Steel. Metals, 2019, 9, 234.	1.0	2
123	Oxidation Behavior of Maraging 300 Alloy Exposed to Nitrogen/Water Vapor Atmosphere at 500 °C. Metals, 2021, 11, 1021.	1.0	2
124	Measuring the fracture toughness of single WC grains of cemented carbides by means of microcantilever bending and micropillar splitting. International Journal of Refractory Metals and Hard Materials, 2021, 98, 105529.	1.7	2
125	Small-scale mechanical response at intermediate/high temperature of 3D printed WC-Co. Procedia CIRP, 2022, 108, 507-512.	1.0	2
126	Tailorable Nanoporous Hydroxyapatite Scaffolds for Electrothermal Catalysis. ACS Applied Nano Materials, 2022, 5, 8526-8536.	2.4	2

#	Article	IF	CITATIONS
127	Novel Procedures for the Microstructural Design of SOFC Materials. ECS Transactions, 2009, 25, 567-576.	0.3	1
128	Nano-mechanical properties of silver-welded YBCO bulks. Journal of Physics: Conference Series, 2010, 234, 012034.	0.3	1
129	Low Sr doping effects on critical current density and pinning mechanism of YBa ₂ Cu ₃ O _{7-1̂} single crystals. Journal of Physics: Conference Series, 2014, 568, 022014.	0.3	1
130	Functional behavior of the anomalous magnetic relaxation observed in melt-textured YBa2Cu3O7-Î ⁷ samples showing the paramagnetic Meissner effect. Physica C: Superconductivity and Its Applications, 2016, 529, 44-49.	0.6	1
131	Contact fatigue behaviour of CVD coated cemented carbides in dry and wet conditions. Wear, 2022, 492-493, 204215.	1.5	1
132	Magnetical Response and Mechanical Properties of High Temperature Superconductors, YBaCu3O7-X Materials. , 0, , .		0
133	Chemically Introduced Disorder Effects on the Critical Current Density and Pinning Mechanisms of \${YBa}_{2-x}{Sr}_{x}{Cu}_{3}{O}_{7-delta}\$. IEEE Transactions on Applied Superconductivity, 2016, 26, 1-4.	1.1	0